A Combined Electrochemical Quartz-Crystal Microbalance Probe Beam Deflection (EQCM – PBD) Study of Solvent and Ion Transfers at a Poly[Ni(saltMe)]-Modified Electrode During Redox Switching**

M. Vilas-Boas,[a] M. J. Henderson,[b] C. Freire,*[a] A. R. Hillman,*[b] and E. Vieil[c]

Abstract: The oxidative polymerisation of the complex2,3-dimethyl-*N*,*N*′-bis-(salicylidene)butane-2,3-diaminatonickel(II), [Ni(saltMe)], was monitored by the electrochemical quartz microbalance (EQCM) and crystal impedance techniques. Polymerisation efficiency was maintained throughout deposition of a film, which behaved rigidly, on the electrode. A combined EQCM – PBD (probe beam deflection) study of the redox process of the film exposed to a monomer-free solution of 0.1M tetraethylammonium perchlorate (TEAP) in acetonitrile showed an electroneutrality mechanism dominated by anion movement accompanied by co-transfer of solvent above 0.8 V. The individual contributions of all the mobile species involved in the redox switching of the poly[Ni(saltMe)] film were determined quantitatively by temporal convolution analysis; the estimated solution-phase diffusion coefficient of the exchanged species was 1.24×10^{-5} cm^2 s^{-1}.

Keywords: electroactive polymers · ion transfer · nickel · quartz-crystal microbalance · redox chemistry · solvent transfer

Introduction

Nickel(II) complexes based on tetradentate 'N_2O_2' Schiff base ligands derived from salicylaldeyde are known to undergo an irreversible oxidation in solvents of low donor number, such as acetonitrile, to form polymer films at the electrode surface.[1–12] This behaviour contrasts with that observed in strong-donor solvents, such as DMF and $(CH_3)_2SO$, where the complexes undergo a reversible diffusion-controlled Ni^{II} – Ni^{III} oxidation with formation of six-coordinate complexes with two solvent molecules axially coordinated.[13–16]

Several groups[1–5, 17] have characterised electrogenerated [M(salen)]-based polymers (salen = *N*,*N*′-bis(salicylidene)-ethylenediamine dianion). Their efforts focused on the electropolymerisation process, polymer structure, identification of the redox couples and the mechanism of electron transport. We have characterised poly[Ni(salen)] spectroelectrochemically and have shown that the polymer, although based on a bona fide coordination compound, behaves like a polyphenylene, as no electrochemical activity was detected for the bridging nickel centres.[10] Although the latter study provided very important insights into the nature of the surface redox couple and charge carriers, the kinetics of the charge propagation could not be studied because of the limited stability of poly[Ni(salen)]. Recently, we prepared the related monomer [Ni(saltMe)], which has also been polymerised at a platinum electrode in CH_3CN/0.1M tetraethylammonium perchlorate (TEAP).[12] The polymer exhibited two reversible electrochemical processes ($E_{1/2}$(I) = 0.65 V; $E_{1/2}$(II) = 0.91 V) within the potential range 0.0 – 1.3 V. Compared with poly-[Ni(salen)], this polymer exhibits very high conductivity and much higher stability/durability when exposed to solutions of CH_3CN/0.1M tetraethylammonium perchlorate (TEAP). These characteristics have enabled the kinetics of charge propagation within a polymer based on a Ni^{II} – salen-type complex to be studied by cyclic voltammetry and chronoamperometry for the first time.[12] In situ UV/Vis, FTIR and ex situ EPR spectra also show that polymerisation and redox switching of poly[Ni(saltMe)] are ligand-based processes, as have been found for poly[Ni(salen)].[11]

The product of the diffusion coefficient $D_{CT}^{1/2}$ and the concentration C of the electroactive species has been estimated from cyclic voltammetry and chronoamperometry data[12] for the second electrochemical process in the redox switching. From a comparison of the $D_{CT}^{1/2}C$ values for the

[a] Dr. C. Freire, M. Vilas-Boas
CEQUP/Departamento de Química, Faculdade de Ciências
Universidade do Porto, 4169-007 Porto (Portugal)
Fax: (+351) 2-6082959
E-mail: acfreire@fc.up.pt

[b] Prof. A. R. Hillman, M. J. Henderson
Department of Chemistry, University of Leicester
Leicester LE1 7RH (UK)
Fax: (+44) 116-2525227
E-mail: arh7@le.ac.uk

[c] Dr. E. Vieil
Laboratoire d'Electrochimie Moléculaire
Départment de Recherche Fondamentale sur la Matière Condensée
CEA, 38054 Grenoble Cedex 9 (France)

[**] [Ni(saltMe)] = 2,3-dimethyl-*N*,*N*′-bis(salicylidene)butane-2,3-diaminatonickel(II)

0947-6539/00/0607-1160 $ 17.50+.50/0 *Chem. Eur. J.* **2000**, *6*, No. 7

anodic and cathodic electrochemical reactions, and of their dependence on film thickness, this process was interpreted as passage of ClO_4^- and CH_3CN between the film and the solution. Furthermore the in situ FTIR study[11] indicated that the perchlorate band had two components: one band at 1100 cm^{-1} that showed no change in intensity or position as the film was oxidised, and a second feature starting at approximately 1091 cm^{-1} at 0.6 V, the intensity of which increased with increasing potential and the frequency decreased by approximately 11 cm^{-1} over 0.6 V. We have assigned the 1100 cm^{-1} feature to ClO_4^- in solution in the thin layer, and the potential-dependent band to ClO_4^- drawn into the film as the polymer is oxidised. The difference in the chemical environments inside the polymer and in the electrolyte solution explains the difference in wavenumber of the asymmetric stretching between the free anions in solution and the anions within the film.

Qualitatively these results all suggest the participation of ClO_4^- and CH_3CN in the charge transfer in poly[Ni(saltMe)]. We have exploited the power of the newly combined electrochemical quartz crystal microbalance and probe beam deflection methodology[18] to study the redox dynamics of this electroactive film based on a nickel(II)–Schiff base complex.

The nanogram sensivity of the electrochemical quartz microbalance (EQCM) technique makes it possible to study the overall reaction and mechanism of an electrochemically driven process. It has been used extensively as a gravimetric probe of population changes following an electrochemical perturbation,[19, 20] for example during electrodeposition,[21–24] polymer dissolution[25–27] and redox switching of metal oxide films[28] and conducting polymers such as poly(aniline)[29] or poly(bithiophene).[30] Probe beam deflection (PBD) involves the measurement of the deflection of a light beam, aligned parallel to the electrode surface, as it crosses a refractive index gradient generated by interfacial reactions. This in-situ technique is a very convenient tool for the study of ion transport and reaction mechanisms. It has been applied to monitor ion transport in electroactive polymers[18, 31–36] and polymer film formation.[37] In contrast with the EQCM, deflection is not significantly perturbed by solvent transfer between the solution and surface film. As a result, the deflectogram obtained is sensitive primarily to the flux of ionic species moving in response to an electrogenerated perturbation at the electrode surface. The complementary responses of the two techniques are therefore exploited by the EQCM–PBD combination, which allows access to the individual solvent and ion flux contributions to the mass transport dynamics, eliminating any question of film history effects associated with the correlation of mass and deflection from sequential experiments. Thus the ion contributions during the redox switching of poly(*o*-toluidine) have been detected qualitatively by EQCM–PBD.[32]

More recently the relationship between responses from the combined instrument was defined quantitatively for the first time using the Ag^+/Ag^0 deposition/dissolution redox process.[18] The analytical protocol, based on temporal convolution analysis, was then applied successfully to monitor quantitatively the transfer of mobile species at the first and second redox steps of a poly(*o*-toluidine) film exposed to perchloric acid solution.[38]

In the present work the combined EQCM–PBD instrument is used to monitor the transfers of mobile species at poly[Ni(saltMe)] films ([Ni(saltMe)] = 2,3-dimethyl-*N*,*N*′-bis(salicylidene)butane-2,3-diaminatonickel(II)) exposed to 0.1M TEAP in acetonitrile. We apply the mathematical tool of temporal convolution analysis to reveal the relationship between the measured current i, the rate of mass change $\dot{M}$ and the beam deflection θ. For the first time, we are able to determine quantitatively the individual contributions of tetraethylammonium (TEA^+), ClO_4^- and CH_3CN to the dynamics in this novel conducting polymer based on a metal–salen complex. Crystal impedance measurements on poly[Ni(saltMe)] formation also demonstrate film rigidity, thereby making it possible to apply the Sauerbrey equation to interpret EQCM frequency responses gravimetrically.

Results and Discussion

Film deposition

Crystal impedance measurements: The Sauerbrey equation requires that a thin film uniformly distributed over the quartz crystal be considered an extension of the crystal. Consequently, a change in the rigidly attached mass ΔM gives rise to a resonant frequency change described[39] by Equation (1),

$$\Delta f = -\left(\frac{2}{\rho v}\right) f_0^2 \frac{\Delta M}{A} \qquad (1)$$

where ρ is the density of the quartz, ν is the wave velocity in quartz and A is the piezoactive area. Upon deposition of a rigid film, the resonance frequency of the crystal will shift to a lower value with no change in the peak admittance. The deposition of a viscoelastic (non-rigid) film, or changes in the viscoelastic properties of an existing film, will result in decreases in both the resonance frequency and the magnitude of the admittance. For an attached mass that is not rigid, the frequency changes will be less than predicted by Equation (1). In the present context mass variations associated with solvent and ion exchange between the film and the bulk solution would then be underestimated. However, if film viscoelastic properties are not dominant, Equation (1) is still valid.[30, 40] To monitor the viscoelastic properties of the poly[Ni(saltMe)] films, we have performed impedance analysis during the film deposition process (Figure 1), and also during redox switching of the film in monomer-free solution (Figure 2). During the deposition process and after each scan, an admittance versus frequency (G_c versus f) spectrum was collected (Figure 1b), and the resonant admittance was checked in order to ensure that decreases in admittance were not higher than 8–10%. The potential window employed in the polymerisation was decreased from 0.0 V ↔ 1.3 V to 0.0 V ↔ 1.1 V to facilitate finer control over the film deposition process. The variation in the maximum frequency during redox switching (Figure 2) was also probed at 0.0–1.3 V to ensure that ingress of ions and/or solvent did not change the viscoelastic properties of the film significantly. The variation in the maximum

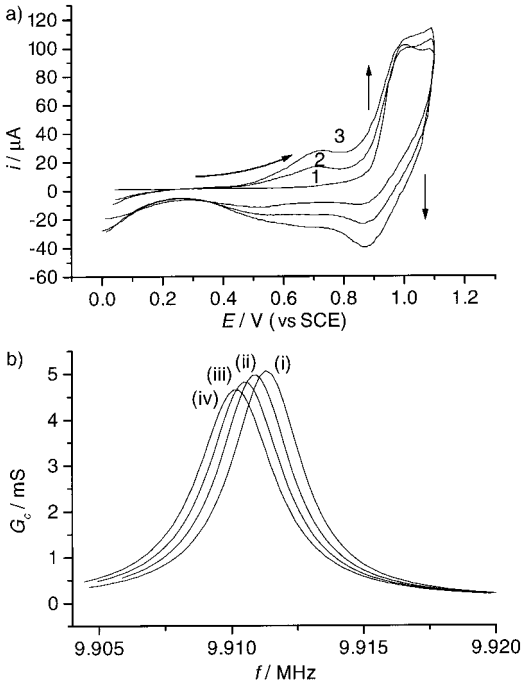

Figure 1. Anodic polymerisation of 1 mM [Ni(saltMe)] in 0.1 M TEAP/CH_3CN at a platinum/quartz-crystal electrode, between 0.0 and 1.1 V at 0.1 $V s^{-1}$: a) i versus E: 1) first, 2) second and 3) third cycle. b) G_c versus f spectra obtained at 0.0 V during the film deposition process: i) bare electrode in 0.1 M TEAP/CH_3CN solution; and after ii) the first cycle, iii) the second cycle and iv) the third cycle.

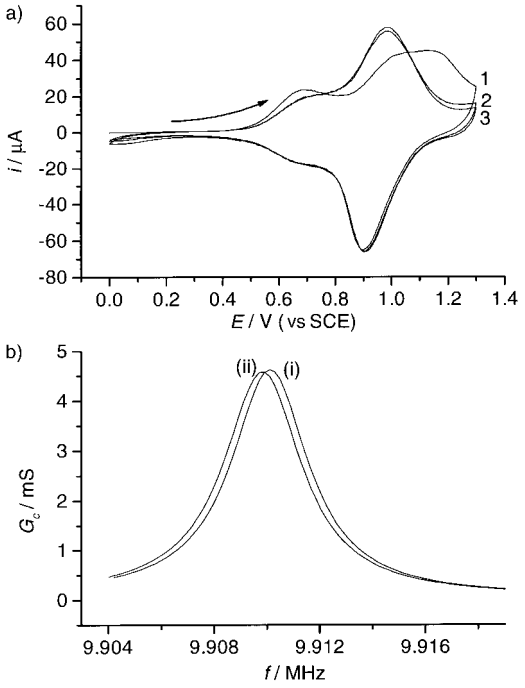

Figure 2. Redox switching of the poly[Ni(saltMe)]-modified electrode in 0.1 M TEAP/CH_3CN between 0 and 1.3 V at 0.1 $V s^{-1}$ ($\Gamma = 11$ nmol cm^{-2}): a) i versus E: 1) first, 2) second and 3)third cycle after polymerisation. b) G_c versus f spectra, collected after a), at: i) 0.0 V and ii) 1.3 V.

admittance between the reduced and oxidised states of the polymer film was less than 1% (Figure 2b); we can therefore interpret the EQCM responses in gravimetric terms.

Gravimetric response: Similar deposition of a poly[Ni(saltMe)] film was monitored by the EQCM; the admittance of the film was checked separately at the beginning and end of the polymerisation process. The data, summarised in Figure 3a, indicate a mass increase commencing at 0.95 V on the first scan, continuing during the reverse scan to 0.9 V and

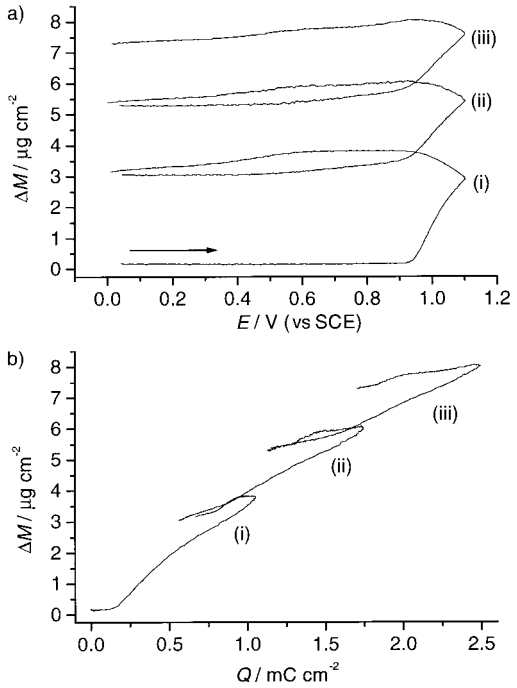

Figure 3. Anodic polymerisation of 1 mM [Ni(saltMe)] in 0.1 M TEAP/CH_3CN at a platinum/quartz-crystal electrode, between 0.0 and 1.1 V at 0.1 $V s^{-1}$: i) first, ii) second and iii) third scan. a) $\Delta M(t)$ versus E; b) $\Delta M(t)$ versus Q for the film deposition. Final film coverage $\Gamma = 11$ nmol cm^{-2}.

thereafter followed by a small mass decrease. This pattern corresponds to the deposition and oxidation of a surface film, followed by film reduction in the last stage of the cathodic half-cycle; this is in accordance with the UV/Vis characterisation of poly[Ni(salen)] film deposition.[10] On the second and third scans there is an earlier mass increase, starting at 0.4 V, corresponding to the oxidation of previously deposited film; this occurs at a potential below that of film formation. The plot of mass change versus charge passed (Figure 3b) reveals some other important features related to the deposition process. The mass increase starts at 0.95 V after some charge has passed. This potential corresponds, in the cyclic voltammetric experiment, to half of the peak current height, indicating a faradaic process at the electrode surface. We may attribute this charge, although not unequivocally, to the first steps of oxidation: monomer oxidation to produce a radical cation, its coupling with monomer and/or other radical cations and supersaturation with polymer in the solution in the vicinity of the electrode. Nucleation of polymer on the surface would follow, leading to the initial abrupt increase in mass.

Linearity of the mass–charge plot observed after the first 500 $\mu C cm^{-2}$ of charge passed would imply that the film was rigid, of constant composition (with respect to film thickness) and produced by processes with a constant faradaic and

0947-6539/00/0607-1162 $ 17.50+.50/0 *Chem. Eur. J.* **2000**, *6*, No. 7

deposition efficiency. The departure from linearity observed, although it is not extreme, indicates that any one or more of these special conditions is violated.

The quantity of charge passed and the mass variation during polymer reduction both increase with the number of polymerisation scans, confirming that more film material is deposited at the electrode surface with each successive scan.

Polymer redox switching

Electrochemical, gravimetric and optical responses: Simultaneous voltammetric, EQCM and PBD responses during the first redox switching cycle of the polymer film were recorded (Figure 4) and profiles were also obtained for a set of three

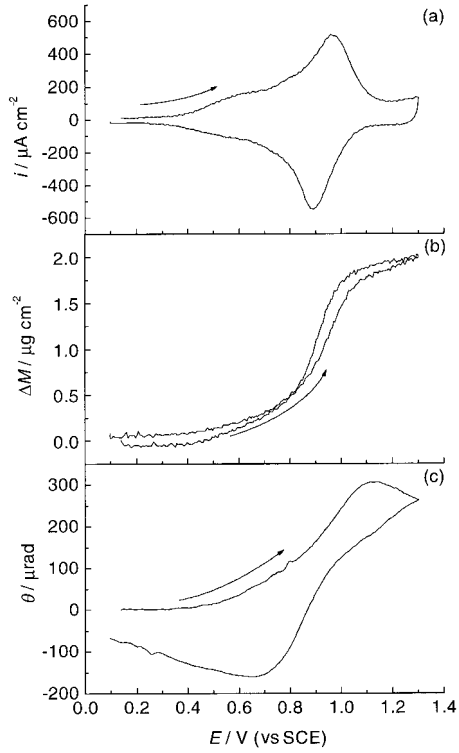

Figure 4. Redox switching of poly[Ni(saltMe)]-modified electrode ($\Gamma =$ 17 nmol cm^{-2}), in 0.1 M TEAP/CH_3CN between 0 and 1.3 V at 0.1 V s^{-1}: a) $i(t)$, b) $\Delta M(t)$ and c) θ. Distance of laser beam from the electrode $x_0 =$ 106 μm (determined experimentally; see text).

scans, in each case after a 30 s hold time at 0.0 V, in order to define the initial PBD and EQCM signals as zero. The quartz crystal – laser beam were calculated by convolution analysis to be 106 μm apart (see below). The reversible electrochemical response (Figure 4a) is typical of that observed previously:[12] a reproducible cyclic voltammogram with two couples, at $E_{1/2}(\mathrm{I}) = 0.65$ and $E_{1/2}(\mathrm{II}) = 0.91$ V.

There is a monotonic mass gain from 0.4 to 1.1 V during the anodic sweep of the polymer (Figure 4b), after which the mass remains constant until 1.3 V; a similar pattern is evident during the cathodic sweep. The $\Delta M - E$ curve does not show significant hysteresis, in accordance with a reversible redox process in which mobile species do not interact strongly with the polymer film.

In the plot of ΔM versus Q for the second redox switching cycle of poly[Ni(saltMe)] (Figure 5), two regions with different slopes can be observed: region I, from 0.4 to 0.8 V (0 – 0.5 mC cm^{-2}) and region II, from 0.8 to 1.3 V (0.5 – 1.1 mC cm^{-2}). The slopes of mass – charge plots for several EQCM experiments on a poly[Ni(saltMe)] film (that of Figure 3; $\Gamma = 11$ nmol cm^{-2}), performed at different scan rates in TEAP/CH_3CN and $TEAPF_6/CH_3CN$ solutions, are analysed in Table 1.

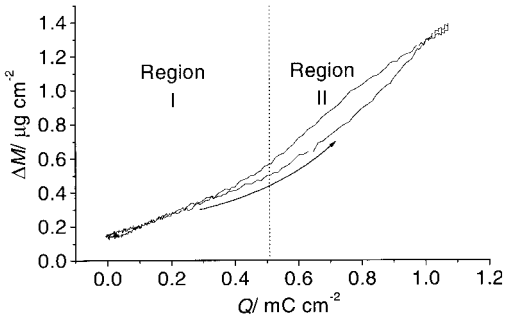

Figure 5. ΔM versus Q profile obtained during the redox switching of the poly[Ni(saltMe)]-modified electrode of Figure 3. $\nu =$ 0.1 V s^{-1}. Region I: 0 – 0.9 V; region II: 0.9 – 1.3 V.

Table 1. Values of the effective molar mass, m, obtained from the slopes of the ΔM versus Q plots for the oxidative redox switching of a poly-[Ni(saltMe]-modified electrode at different scan rates in 0.1 M TEAP/CH_3CN or in 0.1 M $TEAPF_6/CH_3CN$ solutions. Region I: 0 – 0.9 V; region II: 0.9 – 1.3 V.

ν [V s^{-1}]	TEAP m [g mol^{-1}]		$TEAPF_6$ m [g mol^{-1}]	
	I	II	I	II
0.5	73	189	107	232
0.2	80	174	127	214
0.1	70	176	125	224
0.05	60	159	147	241
0.02	63	147	135	229

The effective molar mass, m, of the species exchanged during redox switching was estimated from the slopes; m is defined as $zF\Delta M/Q$, where z is the ion valency, F the Faraday constant and $\Delta M/Q$ the slope obtained from the measured changes in mass M and charge Q.

These data are discussed in detail below, but we note here that the two slopes for the oxidation process in regions I and II do not correspond to Faraday's Law values for pure anion transfers (99.5 g mol^{-1} for perchlorate and 145.0 g mol^{-1} for hexafluorophosphate). We therefore conclude that cation and/or solvent transfers must accompany the anion transfer.

The separation of the ion and solvent contributions, however, cannot be determined easily from the EQCM response alone, because ΔM reflects simultaneous ion and solvent exchange.

The probe beam deflection response, registered with the current and mass variations, is shown in Figure 4c. During oxidation of the film a positive deflection (towards the bulk solution) was detected, a consequence of a decrease in ion concentration at the electrode surface. The beam deviation reaches a maximum at 1.13 V, after which it decreases to a

maximum negative deflection at 0.66 V during reduction, corresponding to an increase in ion concentration at the electrode surface. The delay in the maximum optical signal intensity is clearly evident from qualitative comparison of the potential at which it occurs with those of the maximum electrochemical and gravimetric responses. This delay is a result of the diffusion of the exchanged species between the modified electrode and the light beam located, in this experiment, 106 μm from the electrode.

Convolution analysis: The effect of the propagation delay between the current and mass responses at the electrode surface and the response from the PBD can be overcome by convolution analysis.[34, 41] Assuming semi-infinite diffusion of an ion perpendicular to the electrode surface, the beam profile can be predicted from a measured current response and/or from the EQCM response, expressed as a rate of mass change, $\dot{M}$.[18] The mathematical analysis considers that at any time t the flux $J_A(0, t)$ of an ion species A at the electrode can be linked to the flux $J_A(x, t)$ where the beam is located, by convolving the current or $\dot{M}$ response with the appropriate convolution function $F(x, t)$ [Eq. (2)].[32–34, 38, 42]

$$J_A(x, t) = F(x, t) * J_A(0, t) \quad (2)$$

The function $F(x, t)$ allows a theoretical description of the flux density as a function of time (Equation (3), where D [$cm^2 s^{-1}$] is the coupled diffusion coefficient of the transferred species and its associated co-ion, and x [cm] is the distance from the beam to the electrode surface). The only adjustable parameter in the expression is the ratio $x/(D)^{1/2}$.

$$F(x, t) = \frac{x}{2\sqrt{\pi D t^3}} e^{\frac{-x^2}{4Dt}} \quad (3)$$

A measured current $i(t)$ can be converted into a beam deviation signal at x by Equation (4),[18] where h_k is defined by Equation (5) and k refers to exchanged TEA^+ or ClO_4^-; h_k

$$\theta(x, t) = -\frac{h_k L}{z_k F A} F(x, t) * i(t) \quad (4)$$

$$h_k = \frac{1}{n}\frac{dn}{dc}\frac{1}{D_k} \quad (5)$$

represents the scaling factor that enables the measured $i(t)$ response to be compared with a deflection. With this expression the propagation delay caused by diffusion of ions between the electrode and the laser beam is removed, allowing a quantitative comparison of the electrochemical, gravimetric and optical responses.

Figure 6a shows the PBD responses obtained at several distances from the electrode surface. The delay increases as the distance of the light beam from the electrode is increased, and is seen as a progressive shift along the time axis of the response. The good correlation obtained between the beam deviation and the convolved current (Figure 6b), assuming that the ClO_4^- ions are the only transferred ions responsible for the measured $i(t)$, confirms that perchlorate is the main carrier species responsible for charge compensation during the redox switching of the polymer film.

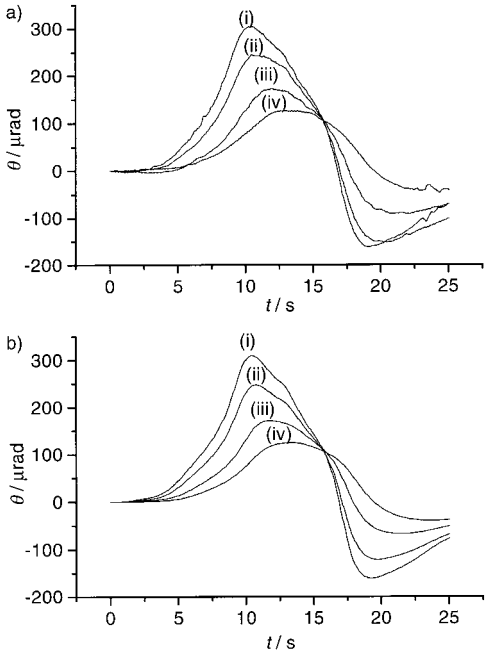

Figure 6. a) Beam deflection response θ versus t; b) convolved current $i(x, t)hL/zFA$ versus t, obtained from the redox switching of the poly-[Ni(saltMe)]-modified electrode of Figure 4 at: i) x_0, the minimum distance of approach; ii) $x_0 + 20$ μm; iii) $x_0 + 40$ μm; iv) $x_0 + 80$ μm.

D_{TEAP} and x_0, the minimum approach distance between the electrode and laser beam, were evaluated by plotting the $x/(D)^{1/2}$ parameter, obtained from the best fit between a convolved current and the experimental beam deviation at several distances from the electrode surface, against the relative beam distance;[18] a typical plot is shown in Figure 7.

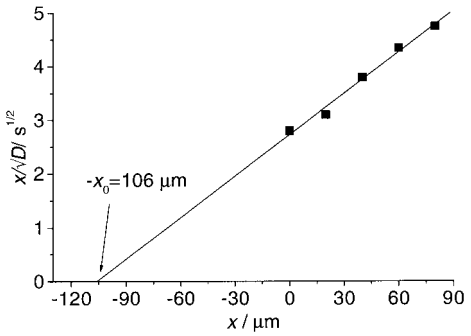

Figure 7. The parameter $x/(D)^{1/2}$ as a function of the relative beam position during redox switching of the poly[Ni(saltMe)]-modified electrode of Figures 4 and 6.

Extrapolation to $x/(D)^{1/2} = 0$ gives $x_0 = 106$ μm. A diffusion coefficient of 1.24×10^{-5} $cm^2 s^{-1}$ is obtained from the slope. We could not find a literature value of D_{TEAP}; however, an approximate value for the coupled diffusion coefficient can be obtained with the Stokes–Einstein equation (Equation (6), where D is the diffusion coefficient, k the Boltzmann

$$D = \frac{kT}{6\pi r\eta} \quad (6)$$

constant, T the temperature, η the solution viscosity and r the radius of the diffusing species).[43] The viscosity of the

0947-6539/00/0607-1164 $ 17.50+.50/0 Chem. Eur. J. 2000, 6, No. 7

electrolyte solution at 25 °C was 0.3694 mPa s.[44] The crystallographic radii, $r_{TEA^+} = 0.377$ nm[45] and $r_{ClO_4^-} = 0.234$ nm[46] seem to be good approximations for r since the cation TEA^+ is not solvated in acetonitrile[47] and the anion ClO_4^- has little or no solvation sphere.[47, 48] Thus D_{TEAP} was determined to be 0.9×10^{-5} cm^2 s^{-1}, in acceptable agreement with our experimental result.

Figure 8 shows the beam deviation profile, convolved current and convolved rate of mass change obtained for three successive cycles at $x = 89$ μm. Except for a fairly small deviation observed between 0 and 0.9 V, the convolved

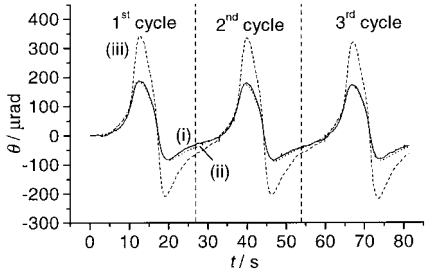

Figure 8. Comparison of i) θ (solid line), ii) convolved current $i(x,t)$ (dotted line) and iii) convolved mass variation $\Delta M(x,t)$ (broken line), for three successive redox cycles of the poly[Ni(saltMe)]-modified electrode of Figures 1 and 2. The representation of time, rather than potential, allows a better visualisation of all the profiles during a complete set of experiments. Distance of laser beam from the electrode $x_0 = 89$ μm.

current (dotted line) is superimposed on the experimental deflection profile (solid line) throughout all the sweeps. This small deviation can only be a result of an ionic species moving in the opposite direction to the perchlorate ion, and must be due to cation egress from the film during oxidation. The expulsion may explain the lower effective mass calculated from the slopes in region I of the mass–charge plots (see Table 1). The higher effective molar mass observed in region II of the plots of ΔM versus Q can be explained by concomitant uptake of solvent with anion. This is in agreement with the higher calculated deflection obtained from the convolved $\dot{M}$ (broken line).

Comparison of the projected $i(t)$ and $\dot{M}$ responses with the experimentally determined PBD profile allows the evaluation of the individual cation, anion and solvent contributions to the overall mobile species transfer process. The protocol for quantitative comparison of all the experimental responses involves convolving $i(t)$ and $\dot{M}$ with the same scaling factor, h_k.[18] Use of the same h_k value, however, takes account of only the anion contribution. The analysis of the $\Delta M/Q$ slopes (Table 1), however, indicates that the ClO_4^- ion transfer is accompanied by solvent movement, so to obtain a more correct h_k value, the ratio of the slope obtained in region II of the plot of ΔM versus Q to the molar mass of the anion was evaluated. A corrected scaling factor was then obtained by matching the ratio (at maximum deflection) between the two convolved signals, mass/current, with that obtained previously. The anion contribution is obtained directly from the integral beam deflection response and the cation contribution is obtained from the difference between the beam deflection response and the convolved current by the protocol previously described.[18, 38] Then the solvent contribution can be obtained by subtracting the anion contribution from the convolved mass variation.

From the resolved contributions (Figure 9), as noted, at the outset of polymer oxidation the electroneutrality of the film is maintained predominantly by the insertion of ClO_4^- into the film. However, a small contribution from the egress of TEA^+ is evident. The solvent swelling of the polymer occurs only for

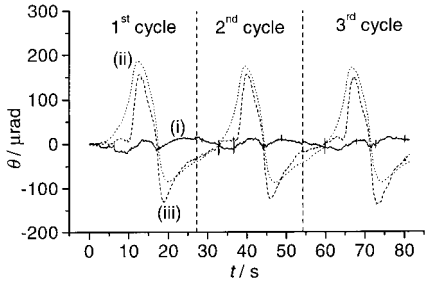

Figure 9. Comparison of: i) cation (solid line), ii) anion (dotted line) and iii) solvent (broken line) contributions to the transfer process at a poly[Ni(saltMe)]-modified electrode calculated as θ versus t, for three sucessive redox cycles between 0 and 1.3 V. Distance of light beam from the electrode $x_0 = 89$ μm. Data from Figure 8.

potentials above 0.8 V and reaches a maximum at 0.95 V on the reverse scan. At that potential the anion and solvent start to leave the film. The tracking of the anion by the solvent for potentials above 0.8 V during film oxidation suggests anion solvation. Perchlorate ion, however, is little solvated in acetonitrile,[47, 48] thus suggesting that the solvent transfer is a result of either a concentration gradient or the entry/exit resulting from simple physical opening/closing of the polymer during redox switching. The polymer swelling above 0.8 V is corroborated by chronoamperometric data in which the values for $C(D_{CT})^{1/2}$ at 0.8 V are lower than that at 1.3 V,[12] suggesting negligible solvent transfer below 0.8 V.

The resolved contributions of cation, anion and solvent (Figure 9) allow the first-cycle effect to be studied. When a 30 s hold time at 0.0 V was applied to the polymer before the set of three cycles, a higher ClO_4^- contribution (dotted line) was obtained for the first cycle than for subsequent ones. This pattern for a set of three cycles was reproducible. These results suggest that the film expels all of the ClO_4^- only when a hold time is applied at the lower potential limit, that is, when the film is completely reduced. At the end of the first and second cycles there is no hold time and the film retains a small amount of ClO_4^-. A break-in effect was also observed for poly(*o*-toluidine),[32, 49] poly(aniline)[29] and poly(vinylferrocene).[50]

The contributions of all the species involved in redox switching can be also expressed in integral form; Figure 10 shows a plot of $\Delta M(x, t)$ versus E for the first cycle of Figure 9. The overall contribution of the solvent corresponds to approximately two solvent molecules per anion. This value agrees with the slope obtained for region II of the plot of ΔM versus Q in Figure 5.

To gain more information on the contribution of the anion to the redox process, plots of ΔM versus Q were recorded for

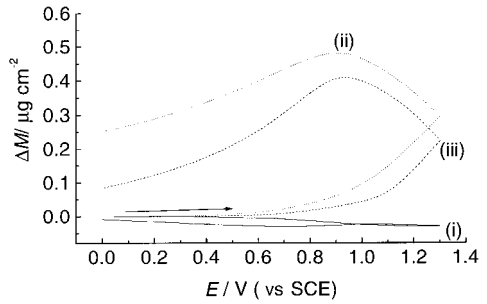

Figure 10. Comparison of: i) cation (solid line) ii) anion (dotted line) and iii) solvent (broken line) contributions for the first oxidative redox switching in Figure 9, calculated as $\Delta M(x, t)$ of i) convolved electrochemical charge $QM_{ClO_4^-}/zFA$; ii) integral beam deflection $\int QM_{ClO_4^-}/zFAhL$; iii) convolved mass variation $\Delta M(x, t)$.

the same concentration of electrolyte but with an anion of different molar mass. The slopes obtained for region II in $TEAPF_6$ also indicate that approximately two solvent molecules are co-transferred per anion (Table 1). The cation contribution appears to be time-dependent, with the electroneutrality of the polymer in region II satisfied by the entry of anion only at slow scan rates; the slopes reach the expected molar mass of the PF_6^- ion.

Concluding Remarks

Poly[Ni(saltMe)] films were deposited onto platinum/quartz-crystal electrodes and the deposition process was studied by microgravimetry. The rigidity of the films was monitored by crystal impedance; the data show the absence of viscoelastic effects that could prejudice the gravimetric interpretation of EQCM frequency changes.

The complementarity of the responses from the combined EQCM – PBD technique has made it possible for the first time to describe the mobile species involved in the redox switching of the novel conducting polymer based on a nickel – Schiff base complex. The study confirmed the occurrence of polymer swelling, and perchlorate ion as the predominant species responsible for maintaining the electroneutrality of the film during the redox switching. It was also possible to conclude that co-ion is involved peripherally, which has not yet been demonstrated by other techniques used to characterise the p-doping of poly[Ni(saltMe)] films.

The individual contributions of cation, anion and solvent were obtained by comparing the electrochemical, gravimetric and optical signals using temporal convolution analysis. The mechanism was found to involve simultaneous expulsion of TEA^+ and uptake of ClO_4^- during the first oxidative step, up to $E_{1/2} = 0.65$ V in the cyclic voltammogram. During the second process, anion uptake is still the major ion contribution, but there is significant solvent entry tracking the anion uptake profile. The solvent appears to be associated with conformational relaxation of the polymer rather than with solvation of the ClO_4^- ion. Quantitative evaluation of the transferred species showed that approximately two molecules of solvent were involved per anion transfer.

Experimental Section

Chemicals: The complex 2,3-dimethyl-*N*,*N*′-bis(salicylidene)butane-2,3-diaminatonickel(II), [Ni(saltMe)], was prepared by a literature procedure,[16] then recrystallised from acetonitrile. TEAP (Fluka, puriss.) and $TEAPF_6$ (Fluka, puriss.) were dried at 60 °C before use. Acetonitrile (Fisons, HPLC grade) was refluxed over CaH_2 and distilled under argon. The acetonitrile – TEAP solutions used in EQCM – PBD experiments were filtered with a 0.1 μm PTFE membrane (Whatman) to remove microscopic solid particles that could scatter the laser beam.

Instrumentation

Electrochemistry: Electrochemical measurements were performed on a custom-built Scanning Ministat II potentiostat (Sycopel Scientific Ltd.). The electrochemical cell was a 42 mm × 30 mm × 30 mm Teflon cuvette with two quartz windows (diameter 20 mm) centred on two opposite sides of the cell, and sealed with adhesive/sealant (Dow Corning 3145 RTV). The working electrode was a 13 mm diameter 10 MHz AT-cut quartz crystal plated with a platinum film (electrochemical area 0.25 cm^2) and mounted on the end of a 55 mm glass tube (o.d. 13 mm). A 15 mm diameter platinum foil counter-electrode and a saturated calomel reference electrode (SCE) were used. The three electrodes were fixed securely to the cuvette by a Teflon lid.

Crystal impedance: Crystal impedance measurements were performed with a Hewlett Packard HP 8512A network analyser in reflectance mode, as described previously.[30] The admittance data acquisition was computer-controlled by an HP BASIC program running on the network analyser built-in computer.

EQCM – PBD: The home-built EQCM circuit was based on that described previously.[51] The arrangement consisted of a 10 MHz platinum/quartz-crystal working electrode, piezoelectric area 0.22 cm^2, isolated from the mains supply earth. For thin films rigidly coupled to the quartz crystal oscillator, variation of the mass ΔM results in a proportional shift in the oscillation frequency Δf of the system, which is described by the Sauerbrey equation.[39] The calibration experiment, involving Ag electrodeposition,[18] gave a coefficient of 9.1×10^{-8} Hz g^{-1}.

The probe beam deflection apparatus consisted of a 2 mW He – Ne laser ($\lambda = 632.8$ nm, Uniphase Model 1122) with a 0.63 mm beam diameter. The beam was focused to about 80 μm diameter and set parallel to the working electrode, giving a 5 mm interaction length. The cell was mounted on a computer-controlled three-axis translation table, allowing translation and rotation to refine the alignment, distance and parallelism between the working electrode and the laser beam. The absolute position of the probe beam with respect to the electrode surface was obtained as previously described.[18] The detector was a dual silicon-based photodiode (Optilas Model 1243 bi-cell) set back 250 mm from the electrochemical cell, which resulted in a position sensitivity of 0.26 μrad mV^{-1}. The deviation angle of a beam following a pathway with a variable refraction index can be described[31] by Equation (7), where θ denotes beam deviation, L the path

$$\theta = \frac{L}{n}\,\frac{\mathrm{d}n}{\mathrm{d}c}\,\frac{\mathrm{d}c}{\mathrm{d}x} \qquad (7)$$

length over which the beam interacts with the concentration profile dc/dx, and dn/dc the variation of the electrolyte concentration c with the refractive index n. The probe laser beam is deflected towards the region of higher refractive index. For this arrangement a positive deflection (towards the solution) indicates ion incorporation into the film, whereas a negative deflection (towards the working electrode) indicates ion expulsion from the film.

The electrochemical, gravimetric and optical signals were recorded simultaneously by a computer fitted with a Datel PC412A data acquisition card. The entire apparatus was mounted on a steel core breadboard 100 mm thick, isolated from the floor by four pneumatic vibration dampeners.

Procedures: Poly[Ni(saltMe)] films were deposited by cycling the potential of the working electrode, exposed to a CH_3CN solution containing 1.0 mM [Ni(saltMe)] monomer and 0.1 M TEAP, between 0.0 and 1.1 V versus SCE at 0.1 V s^{-1}. The upper limit is lower than previously described[12] for the deposition of these films in order to control the amount of polymer deposited more effectively (see the Film deposition section, above).

0947-6539/00/0607-1166 $ 17.50+.50/0 *Chem. Eur. J.* **2000**, *6*, No. 7

Electroactive polymer surface coverage Γ [nmol cm^{-2}] was calculated from the area under the voltammogram of the film at a slow scan rate, $\nu = 0.02$ V s^{-1}, assuming that one positive charge is delocalised over each monomer unit.[12]

After the electropolymerisation the modified electrode was rinsed thoroughly with dry CH_3CN and all the experiments were performed on films immersed in 0.1M TEAP/CH_3CN or 0.1M $TEAPF_6$/CH_3CN. Before the EQCM – PBD experiment the polymer film was cycled (usually with five sweeps) to obtain a reproducible cyclic voltammogram and to remove monomer from within the film. The potential in the monomer-free experiments was varied between the limits 0.0 and 1.3 V, at 0.1 V s^{-1}.

Acknowledgements

This work was partly supported by the "Fundação para a Ciência e Tecnologia" through Project PBIC/QUI/2137/95. M.V.B. thanks the FCT/Praxis XXI for a fellowship. We thank EPSRC (grant GR/L17597) for financial support) and J. Hambleton and G. Bentley of Sycopel Scientific Ltd. for assistance with the instrumentation.

[1] P. Audebert, P. Capdevielle, M. Maumy, *New J. Chem.* **1991**, *15*, 235 – 237.
[2] P. Audebert, P. Capdevielle, M. Maumy, *Synth. Met.* **1991**, *43*, 3049 – 3052.
[3] P. Audebert, P. Capdevielle, M. Maumy, *New J. Chem.* **1992**, *16*, 697 – 703.
[4] P. Audebert, P. Hapiot, P. Capdevielle, M. Maumy, *J. Electroanal. Chem.* **1992**, *338*, 269 – 278.
[5] C. E. Dahm, D. G. Peters, J. Simonet, *J. Electroanal. Chem.* **1996**, *410*, 163 – 171.
[6] C. E. Dahm, D. G. Peters, *Anal. Chem.* **1994**, *66*, 3117 – 3123.
[7] F. Bedioui, E. Labbe, S. Gutierrezgranados, J. Devynck, *J. Electroanal. Chem.* **1991**, *301*, 267 – 274.
[8] K. A. Goldsby, *J. Coord. Chem.* **1988**, *19*, 83 – 90.
[9] K. A. Goldsby, J. K. Blaho, L. A. Hoferkamp, *Polyhedron* **1989**, *8*, 113 – 115.
[10] M. Vilas-Boas, C. Freire, B. Castro, P. A. Christensen, A. R. Hillman, *Inorg. Chem.* **1997**, *36*, 4919 – 4929.
[11] M. Vilas-Boas, C. Freire, B. Castro, P. A. Christensen, A. R. Hillman, unpublished results.
[12] M. Vilas-Boas, C. Freire, B. Castro, A. R. Hillman, *J. Phys. Chem. B* **1998**, *102*, 8533 – 8540.
[13] B. Castro, C. Freire, *Inorg. Chem.* **1990**, *29*, 5113 – 5119.
[14] M. Carrondo, B. Castro, A. M. Coelho, D. Domingues, C. Freire, J. Morais, *Inorg. Chim. Acta* **1993**, *205*, 157 – 166.
[15] C. Freire, B. Castro, *Polyhedron* **1998**, *17*, 4227 – 4235.
[16] C. Freire, B. Castro, *J. Chem. Soc. Dalton. Trans.* **1998**, 1491 – 1497.
[17] K. A. Goldsby, L. A. Hoferkamp, *Chem. Mater.* **1989**, *1*, 348.
[18] M. J. Henderson, A. R. Hillman, E. Vieil, C. Lopez, *J. Electroanal. Chem.* **1998**, *458*, 241 – 248.
[19] S. Bruckenstein, A. R. Hillman in *Handbook of Surface Imaging and Visualization* (Ed.: A. T. Hubbard), CRC Press, Boca Raton, **1995**, p. 101.
[20] D. A. Buttry in *Electroanalytical Chemistry*, *Vol. 17* (Ed.: A. J. Bard), Marcel Dekker, New York, **1991**, p. 1.
[21] D. Dini, F. Decker, G. Zotti, *Electrochem. Solid State Lett.* **1998**, *1*, 217.
[22] S. L. D. Maranhao, R. M. Torresi, *Electrochim. Acta* **1999**, *44*, 1879 – 1885.
[23] C. Kvarnstrom, R. Bilger, A. Ivaska, J. Heinze, *Electrochim. Acta* **1998**, *43*, 355 – 366.
[24] S. Pruneanu, E. Csahok, V. Kertesz, G. Inzelt, *Electrochim. Acta* **1998**, *43*, 2305 – 2323.
[25] A. R. Hillman, D. C. Loveday, S. Bruckenstein, *Langmuir* **1991**, *7*, 191 – 194.
[26] M. Skompska, A. R. Hillman, *J. Chem. Soc. Faraday. Trans.* **1996**, *92*, 4101 – 4108.
[27] X. B. Wang, J. M. Bonnett, R. Pethig, P. K. Baker, O. L. Parri, A. E. Underhill, *J. Mol. Electron.* **1991**, *7*, 167 – 178.
[28] Y. B. Mo, E. Hwang, D. A. Scherson, *J. Electrochem. Soc.* **1996**, *143*, 37 – 43.
[29] M. Kalaji, L. Nyholm, L. M. Peter, *J. Electroanal. Chem.* **1991**, *313*, 271 – 289.
[30] A. Glidle, A. R. Hillman, S. Bruckenstein, *J. Electroanal. Chem.* **1991**, *318*, 411 – 420.
[31] C. Barbero, M. C. Miras, R. Kotz, *Electrochim. Acta* **1992**, *37*, 429 – 437.
[32] M. J. Henderson, A. R. Hillman, E. Vieil, *J. Electroanal. Chem.* **1998**, *454*, 1 – 8.
[33] C. Lopez, M. F. M. Viegas, G. Bidan, E. Vieil, *Synth. Met.* **1994**, *63*, 73 – 78.
[34] E. Vieil, K. Meerholz, T. Matencio, J. Heinze, *J. Electroanal. Chem.* **1994**, *368*, 183 – 191.
[35] M. ElRhazi, C. Lopez, C. Deslouis, M. M. Musiani, B. Tribollet, E. Vieil, *Synth. Met.* **1996**, *78*, 59 – 66.
[36] E. Csahok, E. Vieil, G. Inzelt, *J. Electroanal. Chem.* **1998**, *457*, 251 – 255.
[37] L. M. Abrantes, J. P. Correia, *Electrochim. Acta* **1999**, *44*, 1901 – 1910.
[38] M. J. Henderson, A. R. Hillman, E. Vieil, *J. Phys. Chem. B* **1999**, *103*, 8899 – 8907.
[39] G. Sauerbrey, *Z. Phys.* **1959**, *155*, 206.
[40] S. Ramirez, A. R. Hillman, *J. Electrochem. Soc.* **1998**, *145*, 2640 – 2647.
[41] E. Vieil, *J. Electroanal. Chem.* **1994**, *364*, 9 – 15.
[42] E. Vieil, 204th ACS Meeting **1992**, *Abstracts of Papers,* 156-COLL.
[43] P. W. Atkins, *Physical Chemistry*, *4th ed.*, Oxford University Press, Oxford, **1990**, p. 765.
[44] C. Franco, J. M. Costa, *An. Quím.* **1985**, *81*, 214 – 218.
[45] E. J. King, *J. Phys. Chem.* **1970**, *74*, 4590.
[46] H. D. B. Jenkins, K. P. Thakur, *J. Chem. Educ.* **1979**, *56*, 576.
[47] J. F. Coetzee, W. R. Sharpe, *J. Solution Chem.* **1972**, *1*, 77.
[48] J. Barthel, R. Deser, *J. Solution Chem.* **1994**, *23*, 1133 – 1146.
[49] M. I. Florit, *J. Electroanal. Chem.* **1996**, *408*, 257 – 259.
[50] A. R. Hillman, N. A. Hughes, S. Bruckenstein, *J. Electrochem. Soc.* **1992**, *139*, 74 – 77.
[51] S. Bruckenstein, M. Shay, *Electrochim. Acta* **1985**, *30*, 1295 – 1300.

Received: June 11, 1999
Revised version: October 25, 1999 [F1845]